Synthesis, Structure, and Supramolecular Architecture of Benzonitrile and Pyridine Adducts of Bis(pentafluorophenyl)zinc: Pentafluorophenyl–Aryl Interactions versus Homoaromatic Pairing

Eddy Martin,[†] Claire Spendley,[†] Andrew J. Mountford,[†] Simon J. Coles,[‡] Peter N. Horton,[‡] David L. Hughes,[†] Michael B. Hursthouse,[‡] and Simon J. Lancaster*,[†]

Wolfson Materials and Catalysis Centre, School of Chemical Sciences and Pharmacy, University of East Anglia, Norwich, NR4 7TJ U.K., and School of Chemistry, University of Southampton, Highfield, Southampton, SO17 1BJ U.K.

Received November 9, 2007

Treatment of $(C_6F_5)_2Zn$(toluene) with 2 equiv of a series of benzonitrile or pyridine derivatives yielded the complexes $(C_6F_5)_2Zn(L)_2$ (where L = benzonitrile, 4-(phenyl)benzonitrile, 4-(*N*-pyrrolyl)benzonitrile, pyridine, 4-(phenyl)pyridine, and 4-(*N*-pyrrolyl)pyridine). The four-coordinate solution-phase nature of these complexes was confirmed by a series of variable-temperature ^{19}F NMR experiments and comparison to $(C_6F_5)_2Zn$(2,2′-bipy). The solvent-free solid-state structures of each of the four-coordinate adducts and the toluene solvate of $(C_6F_5)_2Zn(NCC_6H_4C_6H_5)_2$ were determined by single-crystal X-ray diffraction and have distorted tetrahedral geometries. Analysis of the crystal packing revealed a preponderance of offset face-to-face homo−aryl and embrace-like interactions over the hetero−aryl, pentafluorophenyl−phenyl, interaction. These aryl−aryl synthons serve to assemble paired, one- and three-dimensional supramolecular architectures.

Introduction

The attraction of coordination complexes to supramolecular chemists derives from the combination of highly directional dative bonding and metal ion nodes with geometries not found in organic chemistry.[1] In particular, supramolecular coordination complexes of zinc have received considerable attention, and examples have been considered for applications in nonlinear optics[2] and as gas storage materials.[3,4] While dative bonding continues to dominate supramolecular coordination chemistry, there is now increasing recognition of the role that secondary interactions, such as hydrogen bonding and aryl−aryl pairing, play in determining the three-dimensional assembly of metal complexes.[5] These are the supramolecular synthons familiar to the organic crystal engineer.[1a–c,6] We and others are endeavoring to direct the supramolecular assembly of organometallic complexes using the tools of organic crystal engineering and without recourse to dative bonds.[7–14] Despite the challenges associated with depending upon such weak interactions, this approach promises materials more readily processed than metal organic

* To whom correspondence should be addressed. Fax: 44 1603 592003. Tel: 44 1603 592009. E-mail: S.Lancaster@uea.ac.uk.

[†] University of East Anglia.

[‡] University of Southampton.

(1) (a) Steed, J. W.; Atwood, J. L. *Supramolecular Chemistry*; Wiley: Weinheim, Germany, 2000; (b) Lindoy, L. F.; Atkinson, I. M. *Self-Assembly in Supramolecular Systems*; Cambridge University Press: Cambridge, UK, 2000. (c) Steed, J. W.; Turner, D. R.; Wallace, K. J. *Core Concepts in Supramolecular Chemistry and Nanochemistry*; Wiley: Weinheim, Germany, 2007. (d) Jones, C. *J. Chem. Soc. Rev.* **1998**, *27*, 289. (e) Fujita, M. *Chem. Soc. Rev.* **1998**, *27*, 417. (f) Leininger, S.; Olenyuk, B.; Stang, P. J. *Chem. Rev.* **2000**, *100*, 853. (g) Holliday, B. J.; Mirkin, C. A. *Angew. Chem. Int. Ed.* **2001**, *40*, 2022. (h) Moulton, B.; Zaworotko, M. J. *Chem. Rev.* **2001**, *101*, 1629. (i) Janiak, C. *Dalton Trans.* **2003**, 2781. (j) Schalley, C. A.; Lützen, A.; Albrecht, M. A. *Chem.−Eur. J.* **2004**, *10*, 1072.

(2) (a) Evans, O. R.; Lin, W. *Acc. Chem. Res.* **2002**, *35*, 511. (b) Maury, O.; Le Bozec, H. *Acc. Chem. Res.* **2005**, *38*, 691.

(3) Eddaoudi, M.; Kim, J.; Rosi, N.; Vodak, D.; Wachter, J.; O'Keeffe, M.; Yaghi, O. M. *Science* **2002**, *295*, 469.

(4) Erxleben, A. *Coord. Chem. Rev.* **2003**, *246*, 203.

(5) (a) Beatty, A. M. *Coord. Chem. Rev.* **2003**, *246*, 131. For further examples see: (b) Zhang, X.-M.; Tong, M.-L.; Gong, M.-L.; Chen, X.-M. *Eur. J. Inorg. Chem.* **2003**, 138. (c) Zhang, L.-Z.; Liu, G.-F.; Zheng, S.-L.; Ye, B.-H.; Zhang, X.-M.; Chen, X.-M. *Eur. J. Inorg. Chem.* **2003**, 2965. (d) Zhang, X.-M.; Chen, J.-S.; Xu, K.-Y.; Ding, C.-R.; She, W.-L.; Chen, X.-M. *Inorg. Chim. Acta* **2004**, *357*, 1389. (e) Fasina, T. M.; Collings, J. C.; Lydon, D. P.; Albesa-Jove.; Batsanov, A. S.; Howard, J. A. K.; Nguyen, P.; Bruce, M.; Scott, A. J.; Clegg, W.; Watt, S. W.; Viney, C.; Marder, T. B. *J. Mater. Chem.* **2004**, *14*, 2395. (f) Vázquez, M.; Bermejo, M. R.; Licchelli, M.; González-Noya, A. M.; Pedrido, R. M.; Sangregorio, C.; Sorace, L.; Garcia-Deibe, A. M.; Sanmartin, J. *Eur. J. Inorg. Chem.* **2005**, 3479. (g) Ye, B.-H.; Tong, M.-L.; Chen, X.-M. *Coord. Chem. Rev.* **2005**, *249*, 545.

(6) (a) Desiraju, G. R. *Angew. Chem. Int. Ed. Engl.* **1995**, *34*, 2311. (b) Fraxedas, J. *Molecular Organic Materials: From Molecules to Crystalline Solids*; Cambridge University Press: Cambridge, UK, 2006. (c) Desiraju, G. R. *Angew. Chem. Int. Ed.* **2007**, *46*, 8342.

(7) (a) Braga, D.; Grepioni, F.; Desiraju, G. R. *Chem. Rev.* **1998**, *98*, 1375. (b) Haiduc, I.; Edelman, F. T. *Supramolecular Organometallic Chemistry*; Wiley-VCH: Weinheim, Germany, 1999. (c) Desiraju, G. R. *J. Chem. Soc., Dalton Trans.* **2000**, 3745. (d) Braga, D.; Grepioni, F. *Acc.Chem. Res.* **2000**, *33*, 601. (e) Hosseini, M. W. *Acc. Chem. Res.* **2005**, *38*, 313.

(8) (a) Braga, D.; Maini, L.; Paganelli, F.; Tagliavini, E.; Casolari, S.; Grepioni, F. *J. Organomet. Chem.* **2001**, *637–639*, 609. (b) Braga, D.; Polito, M.; Bracaccini, M.; D'Addario, D.; Tagliavini, E.; Sturba, L.; Grepioni, F. *Organometallics* **2003**, *22*, 2142. (c) Braga, D.; Polito, M.; Bracaccini, M.; D'Addario, D.; Tagliavini, E.; Proserpio, D. M.; Grepioni, F. *Chem. Commun.* **2002**, 1080. (d) Braga, D.; Maini, L.; Polito, M.; Tagliavini, E.; Grepioni, F. *Coord. Chem. Rev* **2003**, *246*, 53. (e) Braga, D.; Polito, M.; D'Addario, D.; Tagliavini, E.; Proserpio, D. M.; Grepioni, F.; Steed, J. W. *Organometallics* **2003**, *22*, 453. (f) Braga, D.; Polito, M.; Grepioni, F. *Cryst. Growth Des.* **2004**, *4*, 769. (g) Braga, D.; Giaffreda, S. L.; Polito, M.; Grepioni, F. *Eur. J. Inorg. Chem.* **2005**, 2737. (h) Braga, D.; Polito, M.; Giaffreda, S. L.; Grepioni, F. *Dalton Trans.* **2005**, 2766.

(9) (a) Mareque Rivas, J. C.; Brammer, L. *Coord. Chem. Rev* **1999**, *183*, 43. (b) Brammer, L.; Mareque Rivas, J. C.; Atencio, R.; Fang, S.; Pigge, F. C. *J. Chem. Soc., Dalton Trans.* **2000**, 3855. (c) Brammer, L. *Chem. Soc. Rev.* **2004**, *33*, 476.

(10) Zakaria, C. M.; Ferguson, G.; Lough, A. J.; Glidewell, C. *Acta Crystallogr., Sect. B* **2002**, *58*, 786.

10.1021/om701127p CCC: $40.75 © 2008 American Chemical Society
Publication on Web 03/05/2008

Scheme 1

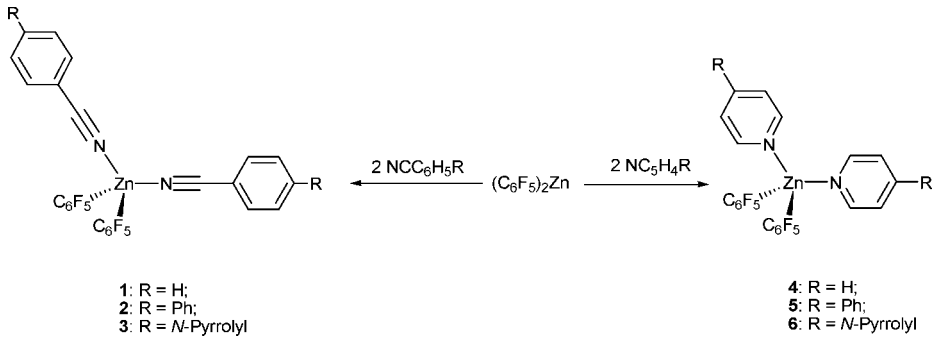

frameworks and with properties more closely related to discrete molecules than coordination polymers.

Interest in pentafluorophenyl complexes originated with the highly electron-withdrawing nature of the group, rendering the metal center highly Lewis acidic.[15] We were initially alerted to the potential of organofluorine groups in supramolecular chemistry by a series of structural and spectroscopic observations revealing significant intramolecular interactions.[16,17] The three most pertinent intermolecular interactions in which the pentafluorophenyl group participates are pairing or stacking with aryl groups, offset face-to-face arrangements with other perfluoroaryl rings, and acting as a hydrogen bond acceptor. The first is perhaps the best known of these prospective supramolecular synthons and results from the opposing quadrupoles of the perfluorophenyl and phenyl groups.[18] Since the original demonstration of the elevation in melting point on mixing benzene and hexafluorobenzene,[19] it has been employed by a number of groups to influence supramolecular assembly.[20–22] There is also a limited number of reports of organometallic compounds exhibiting aryl−perfluoroaryl stacking and pairing interactions.[23,24]

Despite their opposite quadrupole moments, the offset face-to-face (*off*) interaction between perfluoroaromatic groups is comparable to the often observed supramolecular motif in which aromatics form *off* pairs or stacks.[25,26] Such *off* interactions between pairs or stacks of C_6F_5 groups have been reported for organometallic and coordination compounds with pentafluorophenyl substituents.[13,27]

During a study of N−H···F−C hydrogen bonding in protic amine adducts of tris(pentafluorophenyl)-aluminum and -boron we found examples of intramolecular phenyl−pentafluorophenyl pairing interactions.[16d] In order to establish a one-to-one correspondence between the number of C_6F_5 groups and Lewis acidic sites, favoring the formation of infinite supramolecular assemblies, our subsequent investigations have focused upon the supramolecular architectures of adducts of bis(pentafluorophenyl)zinc.[28,29] Determination of the structures of a series of protic amine adducts revealed their assembly through examples of N−H···F−C contacts, *off* phenyl−phenyl (Ph_H···Ph_H) and *off* pentafluorophenyl−pentafluorophenyl interactions (Ph_F···Ph_F), while there were relatively few instances of phenyl−pentafluorophenyl interactions (Ph_H···Ph_F).[28] This was surprising in light of the prominence this interaction has attained in the literature. We concluded that the fine balance between competing intermolecular interactions yielded a series in which no one supramolecular interaction predominated.

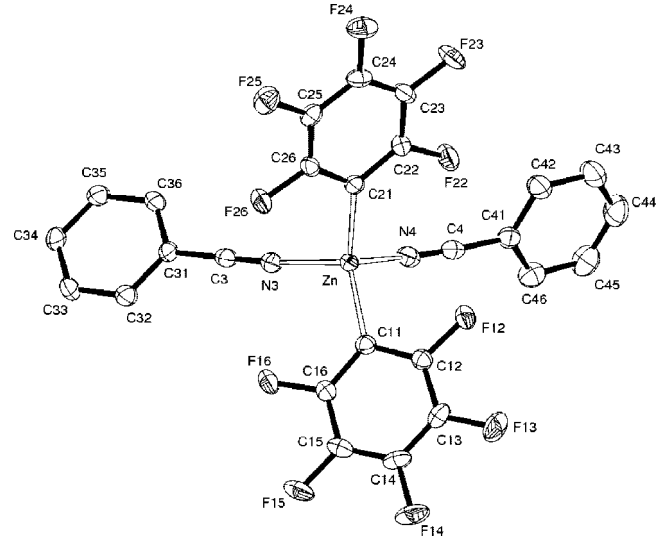

Figure 1. Molecular structure of **1**. Displacement ellipsoids are shown at the 50% probability level. Hydrogen atoms have been omitted for clarity.

(11) (a) Elschenbroich, C.; Lu, F.; Harms, K. *Organometallics* **2002**, *21*, 5152. Elschenbroich, C.; Schiemann, O.; Burghaus, O.; Harms, K. *J. Am. Chem. Soc.* **1997**, *119*, 7452.

(12) Tse, M. C.; Cheung, M. C.; Chan, M. C. W.; Che, C. M. *Chem. Commun.* **1998**, *21*, 2295.

(13) Kim, Y. J.; Verkade, J. G. *Inorg. Chem.* **2003**, *42*, 4262.

(14) (a) Oh, M.; Carpenter, G. B.; Sweigart, D. A. *Organometallics* **2003**, *22*, 2364. (b) Oh, M.; Carpenter, G. B.; Sweigart, D. A. *Angew. Chem. Int. Ed.* **2002**, *41*, 3650. (c) Oh, M.; Carpenter, G. B.; Sweigart, D. A. *Chem. Commun.* **2002**, *18*, 2168.

(15) (a) Piers, W. E.; Chivers, T. *Chem. Soc. Rev.* **1997**, *26*, 345. Erker, G. Dalton Trans. 2005, 1883. (b) Piers, W. E. *Adv. Organomet. Chem.* **2005**, *52*, 1.

(16) (a) Lancaster, S. J.; Rodriguez, A.; Lara-Sanchez, A.; Hannant, M. D.; Walker, D. A.; Hughes, D. L.; Bochmann, M. *Organometallics* **2002**, *21*, 451. (b) Lancaster, S. J.; Mountford, A. J.; Hughes, D. L.; Schormann, M.; Bochmann, M. *J. Organomet. Chem.* **2003**, *680*, 193. (c) Mountford, A. J.; Hughes, D. L.; Lancaster, S. J. *Chem. Commun.* **2003**, 2148. (d) Mountford, A. J.; Lancaster, S. J.; Coles, S. J.; Horton, P. N.; Hughes, D. L.; Hursthouse, M. B.; Light, M. E. *Inorg. Chem.* **2005**, *44*, 5921. (e) Mountford, A. J.; Clegg, W.; Harrington, R. W.; Humphrey, S. M.; Lancaster, S. J. *Chem. Commun.* **2005**, 2044. (f) Mountford, A. J.; Clegg, W.; Coles, S. J.; Harrington, R. W.; Horton, P. N.; Humphrey, S. M.; Hursthouse, M. B.; Wright, J. A.; Lancaster, S. J. *Chem.−Eur. J.* **2007**, *13*, 4535. (g) Mountford, A. J.; Lancaster, S. J.; Coles, S. J. *Acta Crystallogr., Sect. C* **2007**, *63*, m401.

(17) For a review of the supramolecular chemistry of organofluorine see: Reichenbächer, K.; Süss, H. I.; Hulliger, J. *Chem. Soc. Rev.* **2005**, *34*, 22.

(18) (a) Williams, J. H. *Acc. Chem. Res* **1993**, *26*, 593. (b) West, Jr., A. P.; Mecozzi, S.; Dougherty, D. J. *Phys. Org. Chem.* **1997**, *10*, 347. (c) Vanspeybrouck, W.; Herrebout, W. A.; van der Veken, B. J.; Lundell, J.; Perutz, R. N. *J. Phys. Chem. B* **2003**, *107*, 13855.

(19) Patrick, C. R.; Prosser, G. S. *Nature* **1960**, *187*, 1021.

(20) (a) Coates, G. W.; Dunn, A. R.; Henling, L. M.; Dougherty, D. A.; Grubbs, R. H. *Angew. Chem., Int. Ed. Engl.* **1997**, *36*, 248. (b) Coates, G. W.; Dunn, A. R.; Henling, L. M.; Ziller, J. W.; Lobkovsky, E. B.; Grubbs, R. H. *J. Am. Chem. Soc.* **1998**, *120*, 3641. (c) Kilbinger, A. F. M.; Grubbs, R. H. *Angew. Chem. Int. Ed.* **2002**, *41*, 1563. (d) Coates, G. W.; Dunn, A. R.; Henling, L. M.; Ziller, J. W.; Lobkovsky, E. B.; Grubbs, R. H. *J. Am. Chem. Soc.* **2003**, *42*, 3903.

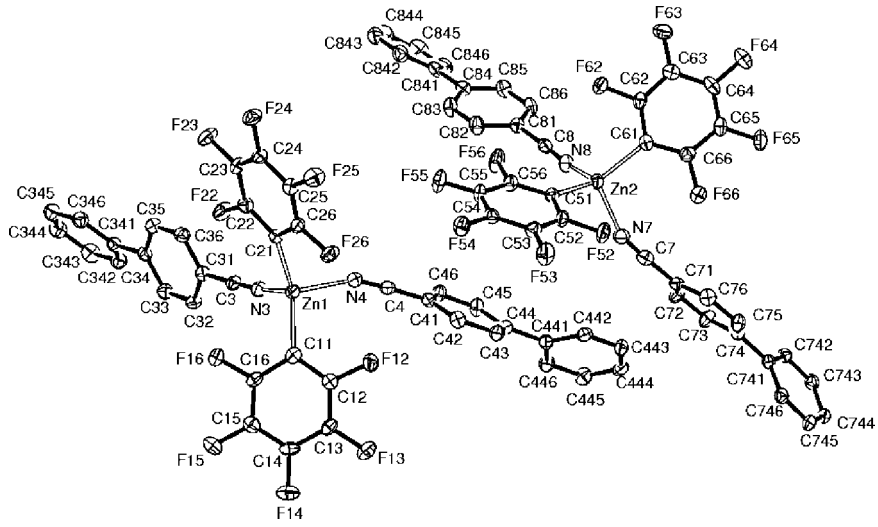

Figure 2. Molecular structures and relative orientations of the two, very similar but crystallographically independent, molecules in the toluene-free lattice of **2**. Displacement ellipsoids are shown at the 50% probability level. Hydrogen atoms have been omitted for clarity.

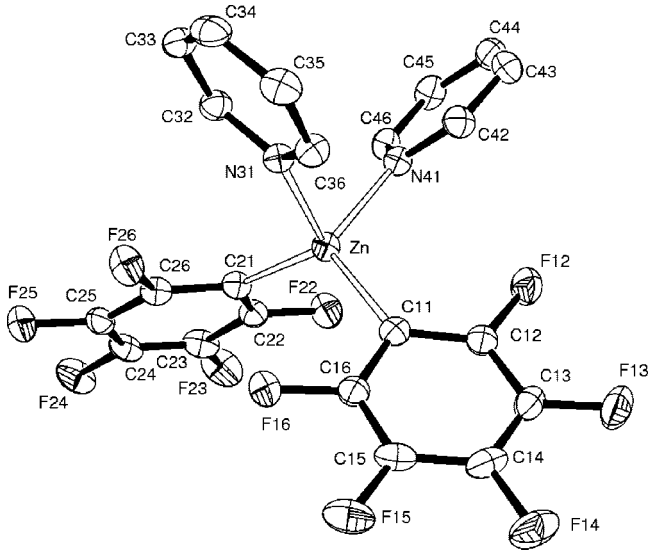

Figure 3. Molecular structure of **4**. Displacement ellipsoids are shown at the 50% probability level. Hydrogen atoms have been omitted for clarity.

We now report the synthesis, structure, and supramolecular architecture of 4-substituted benzonitrile and pyridine adducts of bis(pentafluorophenyl)zinc. The absence of protic hydrogens was intended to simplify the interplay of intermolecular interactions and allow us to determine the relative preference for phenyl−phenyl (**I**), pentafluorophenyl−phenyl (**II**), and pentafluorophenyl−pentafluorophenyl (**III**) interactions in these systems. In addition, while intramolecular aryl-pairing interactions were geometrically possible and occurred in the benzyl amine adducts we reported earlier,[16d] this complication should be absent in the pyridine and benzonitrile adducts.

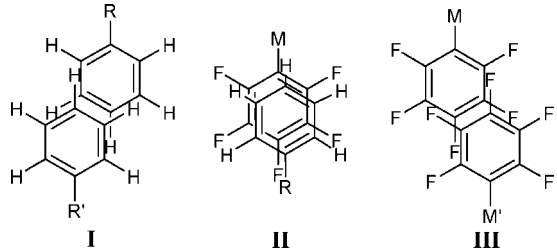

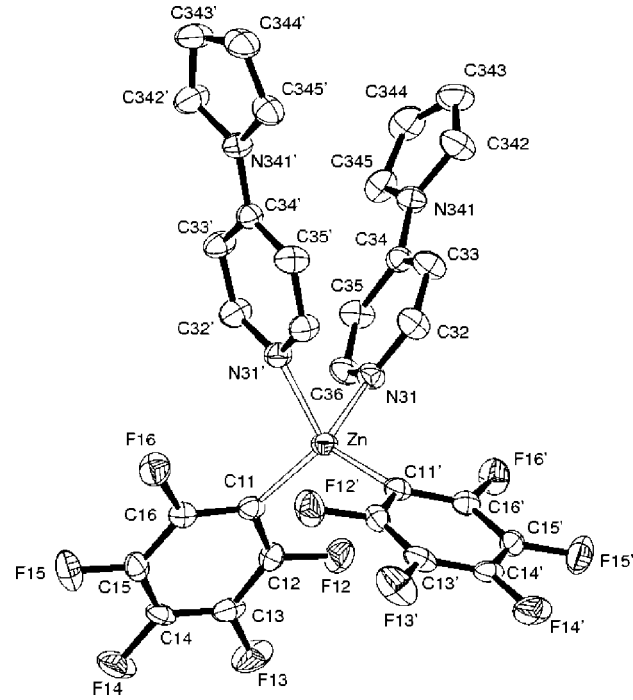

Figure 4. Molecular structure of **6**. Displacement ellipsoids are shown at the 50% probability level. Hydrogen atoms have been omitted for clarity. Compound **6** has a two-fold symmetry axis passing through the zinc atom and is isostructural with compound **5**.

Results and Discussion

Treatment of a toluene solution of $(C_6F_5)_2Zn$ with the appropriate benzonitrile or pyridine donor resulted in conversion to adducts **1**−**6** in excellent yield (Scheme 1), with elemental analyses in good agreement with the expected compositions. As was the case for the previously reported amine adducts of bis(pentafluorophenyl)zinc,[28] the ^1H and ^{19}F NMR data proved indicative of adduct formation. The *ortho*-fluorine resonances are all within ±2 ppm of that for $(C_6F_5)_2Zn$ (–118.3 ppm in C_6D_6, where the species present in solution is presumably an arene adduct).[30] However, the value of $\Delta\delta$ (*m*-F – *p*-F) is a more sensitive indicator of the metal coordination environment and reduces from ca. 8 ppm for $(C_6F_5)_2Zn$(arene) to less than 5

Table 1. Selected Bond Lengths and Angles (in Å and deg) for Compounds 1–6, with Esd's in Parentheses

compound	Zn−C		Zn−N		C−Zn−C	N−Zn−N	Zn−N−C	
1	Zn−C11	2.011(2)	Zn−N3	2.067(2)	129.67(8)	97.47(7)	Zn−N3−C3	171.8(2)
	Zn−C21	2.012(2)	Zn−N4	2.112(2)			Zn−N4−C4	156.7(2)
2 Mol. A	Zn−C11	2.002(4)	Zn1−N3	2.105(3)	135.30(13)	97.41(11)	Zn1−N3−C3	162.1(3)
	Zn−C21	2.002(3)	Zn1−N4	2.110(3)			Zn1−N4−C4	157.2(3)
Mol. B	Zn−C51	2.009(3)	Zn2−N7	2.098(3)	132.68(13)	96.25(12)	Zn2−N7−C7	158.0(3)
	Zn−C61	2.018(3)	Zn2−N8	2.097(3)			Zn2−N8−C8	159.9(3)
2·tol	Zn−C11	2.005(2)	Zn−N3	2.093(2)	128.17(9)	99.11(8)	Zn−N3−C3	157.3(2)
	Zn−C21	2.007(2)	Zn−N4	2.090(2)			Zn−N4−C4	157.7(2)
3	Zn−C11	2.0292(16)	Zn−N3	2.0660(14)	123.55(6)	95.75(6)	Zn−N3−C3	175.60(14)
	Zn−C21	2.0209(15)	Zn−N4	2.1206(15)			Zn−N4−C4	174.76(14)
4	Zn−C11	2.032(2)	Zn−N31	2.0998(13)	120.14(6)	92.97(5)	Zn−N31−C34	178.79(8)
	Zn−C21	2.024(2)	Zn−N41	2.0983(14)			Zn−N41−C44	178.17(8)
5	Zn−C11	2.020(3)	Zn−N31	2.099(2)	118.07(14)	87.91(12)	Zn−N31−C34	161.07(11)
6	Zn−C11	2.018(3)	Zn−N31	2.099(2)	117.45(15)	87.59(13)	Zn−N31−C34	162.68(1)

ppm for each of the adducts.[31] Addition of further donor ligand to NMR samples did not result in duplication of ^{1}H NMR resonances but did produce a chemical shift change, whereas cooling the samples to –80 °C led only to a slight broadening of the resonances. These observations support the assumption that, in solution, these adducts participate in dynamic dissociation−association equilibria with free ligand.

The fact that we normally obtain four-coordinate crystalline adducts from solution suggests, but does not prove, that the bis-donor complex is the major constituent of these equilibria. In order to address this point, we prepared the 2,2′-bipyridine (bipy) adduct, $(C_6F_5)_2Zn(bipy)$ (**7**). The ^{19}F NMR spectrum of **7** is very similar to those of adducts **1**−**6** and almost superimposable upon that of compound **4**, $(C_6F_5)_2Zn(py)_2$. Since the chelating bipy ligand must give rise to a four-coordinate complex, we regard the spectral similarity as further compelling evidence that four-coordinate adducts are the predominant species in solution. Furthermore, treatment of $(C_6F_5)_2Zn$(toluene) with less than 2 equiv of monodentate donor and observation at –60 °C resulted in ^{19}F NMR spectra with multiple C_6F_5 environments suggesting that under these conditions three- and four-coordinate complexes can be spectroscopically distinguished.

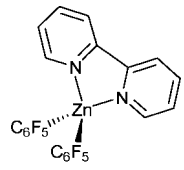

7

Molecular Structures. For compounds **1**, **2**, **4**, and **5**, X-ray quality crystals were afforded by cooling concentrated toluene solutions to –25 °C. Of these, **2** was the only one to crystallize with a solvent molecule in the lattice, giving **2**·toluene. Solvent-free single crystals of **2** and **6** suitable for X-ray diffraction were obtained by layering light petroleum over dichloromethane solutions of the crude products and cooling to –25 °C overnight. The preparation of compound **3**, its crystallization from 1,2-difluorobenzene, and its molecular structure have been communicated and are included here for comparison.[29] The solid-state structures of **1**–**6** and **2**·toluene were determined by X-ray crystallography and are described below. No evidence for the presence of more than one type of crystalline product was observed, under magnification, during the crystal selection process.

Each of the compounds **1**–**6** has the expected essentially tetrahedral ligand coordination about the zinc center (selected ORTEPs are presented in Figures 1, 2, 3, 4). Only compounds **5** and **6** retain the molecular C_2 symmetry axis in the solid state. However, the toluene-free crystal structure of compound **2** is the only example in the series in which there is more than one crystallographically independent molecule in the lattice (for **2**, $Z' = 2$). Selected bond lengths and angles for each member of the series are collated in Table 1.

The Zn−C bond length is a rather insensitive parameter, and there is little variation between complexes in either the benzonitrile (**1**−**3**) or pyridine (**4**−**6**) series of adducts. Indeed, the average Zn−C bond lengths for the benzonitrile, pyridine, and previously reported amine adducts at 2.012, 2.023, and 2.032 Å, respectively, are rather similar. The average Zn−N bond lengths are also remarkably consistent in the benzonitrile (2.096 Å) and pyridine (2.097 Å) adducts; here the greatest variation is observed between asymmetrically coordinated ligands in complexes **1** and **3**. In general, the Zn−N bond lengths are slightly shorter than the bond lengths we observed for amine adducts (2.094−2.187 Å), where the differences reflected more pronounced steric and electronic contrast than is present in the current study.

Whereas there is little variation in the bond length distribution in complexes **1**–**6**, the C−Zn−C angles cover a range of some 12° for the benzonitriles (123–135°), while for the pyridines (117–120°) they are somewhat more acute and cover a smaller range. In contrast, the N−Zn−N angles vary over only 3° for the benzonitriles (96–99°) and cover a slightly wider spread of ca. 6° for the pyridines (87–93°). A number of comparisons suggest that these differences are not simply due to the steric demands of the donor ligands, which should to a first approximation be rather similar. Table 1 lists three significantly different C−Zn−C angles separated by some 7° for compound **2**, two from crystallographically independent molecules in the solvent-free lattice and one from the toluene solvate; the supramolecular origin of these differences is discussed below. The most striking anomaly in Table 1 is the somewhat counterintuitive relationship between the C−Zn−C and N−Zn−N angles. As expected, in each adduct the C−Zn−C angle is the

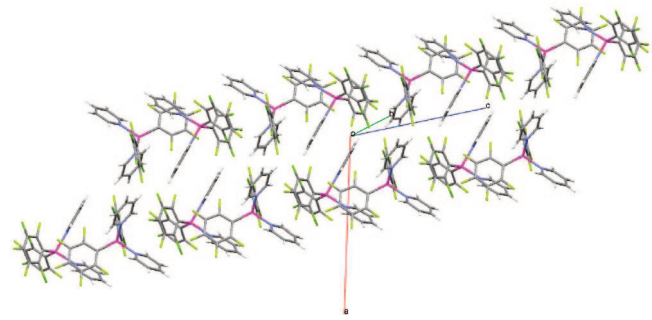

Figure 5. Packing in compound **4**.

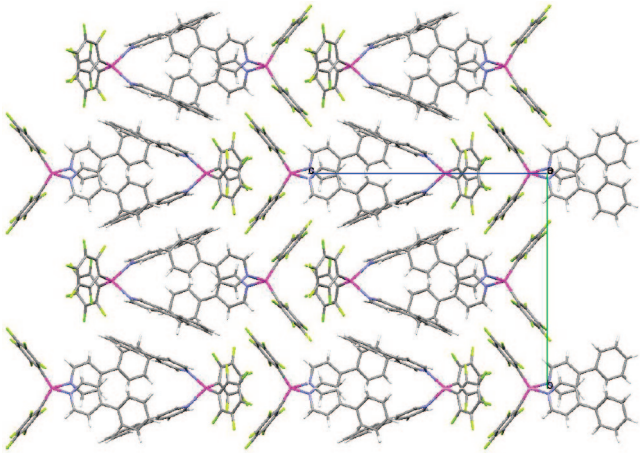

Figure 6. View down the *a* axis, showing the packing in one layer of compound **5**.

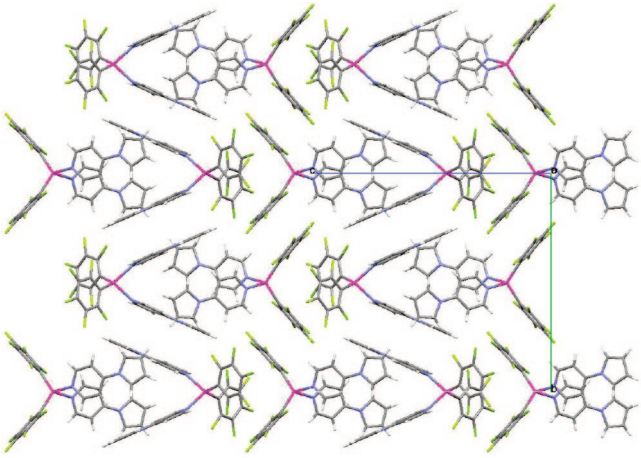

Figure 7. View down the *a* axis of the packing in one layer of compound **6**.

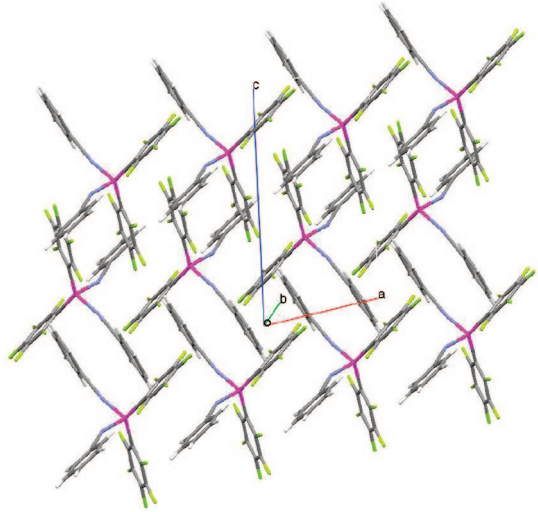

Figure 8. Illustrating the *off* $Ph_H \cdots Ph_H$ and $Ph_F \cdots Ph_F$ stacks in **1** running parallel to the *a* axis.

more obtuse because of the strong repulsion between the pentafluorophenyl groups, while the N−Zn−N is the most acute. From a purely molecular standpoint, it is therefore somewhat surprising that complexes **5** and **6**, which have the smallest C−Zn−C angle distortions from tetrahedral, also exhibit the

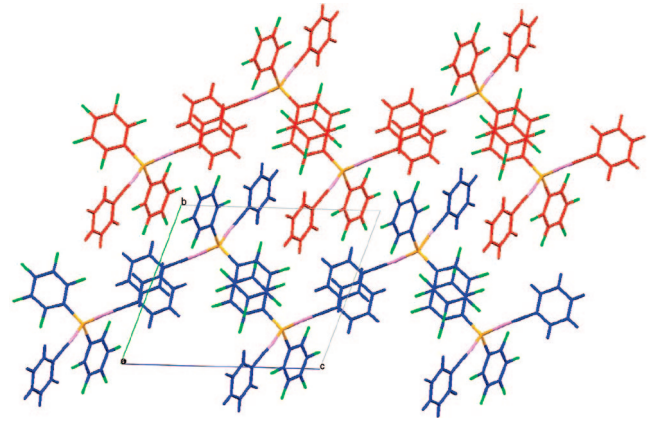

Figure 9. Illustrating the *off* $Ph_H \cdots Ph_H$ and $Ph_F \cdots Ph_F$ pairing interactions, connecting adjacent sheets, in **1**, viewed along the *a* axis. The carbon atoms are colored blue and red to indicate different sheets.

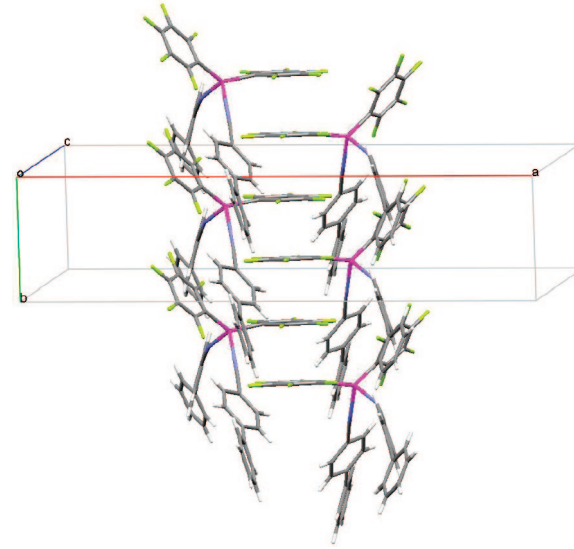

Figure 10. Representation showing pentafluorophenyl rings in a column of molecules of **2A** stacking along a 2_1 symmetry axis.

lowest N−Zn−N angles in the study. More generally, there is not the inverse correlation between C−Zn−C and N−Zn−N angles that might have been anticipated. The Zn−N−C bond angles determined for the benzonitrile adducts also show much greater variation, between 156.7° and 175.6°, than one would initially anticipate. Similarly, the Zn−N−C_{para} angles for the pyridine adducts, which one would also expect to be near linear, cover a range from 161.1° to 178.8°. Further insight into the angular distribution is provided by consideration of these structures as supramolecular assemblies.

(21) (a) Dai, C.; Nguyen, P.; Marder, T. B.; Scott, A. J.; Clegg, W.; Viney, C. *Chem. Commun.* **1999**, 2493. (b) Collings, J. C.; Roscoe, K. P.; Thomas, R. L.; Batsanov, A. S.; Stimson, L. M.; Howard, J. A. K.; Marder, T. B. *New J. Chem.* **2001**, *25*, 1410. (c) Collings, J. C.; Roscoe, K. P.; Robins, E. G.; Batsanov, A. S.; Stimson, L. M.; Howard, J. A. K.; Clark, S. J.; Marder, T. B. *New J. Chem.* **2002**, *26*, 1740. (d) Smith, C. E.; Smith, P. S.; Thomas, R. L.; Robins, E. G.; Collings, J. C.; Dai, C. Y.; Scott, A. J.; Borwick, S.; Batsanov, A. S.; Watt, S. W.; Clark, S. J.; Viney, C.; Howard, J. A. K.; Clegg, W.; Marder, T. B. *J. Mater. Chem.* **2004**, *14*, 413. (e) Collings, J. C.; Smith, P. S.; Yufit, D. S.; Batsanov, A. S.; Howard, J. A. K.; Marder, T. B. *Cryst. Eng. Commun.* **2004**, *6*, 25. (f) Watt, S. W.; Dai, C.; Scott, A. J.; Burke, J. M.; Thomas, R. L.; Collings, J. C.; Viney, C.; Clegg, W.; Marder, T. B. *Angew. Chem., Int. Ed.* **2004**, *43*, 3061. (g) Collings, J. C.; Burke, J. M.; Smith, P. S.; Batsanov, A. S.; Howard, J. A. K.; Marder, T. B. *Org. Biomol. Chem.* **2004**, *2*, 3172.

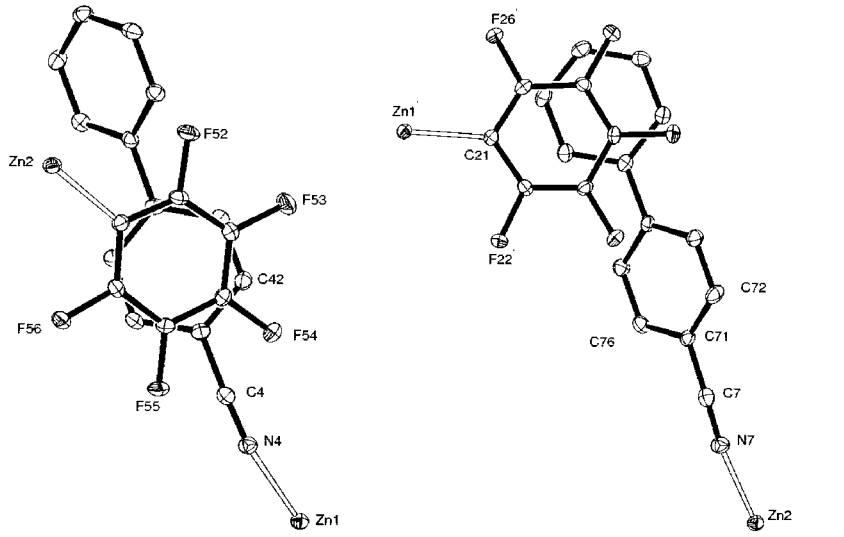

Figure 11. Projection of overlapping rings onto the plane of the lower ring for the pentafluorophenyl−phenyl interactions in **2** (a, b). Displacement ellipsoids are drawn at 30% probability.

Table 2. Hydrogen···Fluorine Contacts

compound	C−H···F	d(H···F)[a] /Å	∠(CHF)/ deg	symmetry operation for intermolecular interaction
2	F52···H72	2.28	150	x, y–1, z
	F26···H46	2.45	140	x, y–1, z
2·(toluene)	F25···H42	2.46	152	2–x, y, 0.5–z
3	F16···H43	2.34	126	x–1, y, z
4	F12···H45	2.46	159	1–x, y–0.5, 1.5–z
	F16···H34	2.42	150	–x, –y, 1–z
5	F13···H32	2.46	129	1–x, y+0.5, 0.25–z
6	F13···H36	2.38	138	–0.5–x, y, 0.75–z

[a] Only those contacts < 2.50 Å are listed here.

Supramolecular Architecture. Adduct **4** has the simplest supramolecular architecture in this study. There are no infinite structural elements, and this is the only example in which there are no offset face-to-face homoaryl interactions between C_6F_5 rings (*off* $Ph_F \cdots Ph_F$). Instead noteworthy supramolecular features are restricted to an *off* interaction between two centrosymmetrically related pyridine ligands (Figure 5).

The packing of **5** is depicted in Figure 6. Molecules of **5** are paired through a 4-fold pentafluorophenyl embrace (FP_FE) of the sort documented by Dance and co-workers.[25] Each molecule is related to its partner by a $\bar{4}$ center where four C_6F_5 ligands are closely bound. The (4-phenyl)pyridine ligands also appear to form an embrace, but this is essentially a shape-based intermeshing, allowing close packing of the molecules; with no short interligand contacts between the four ligands involved,

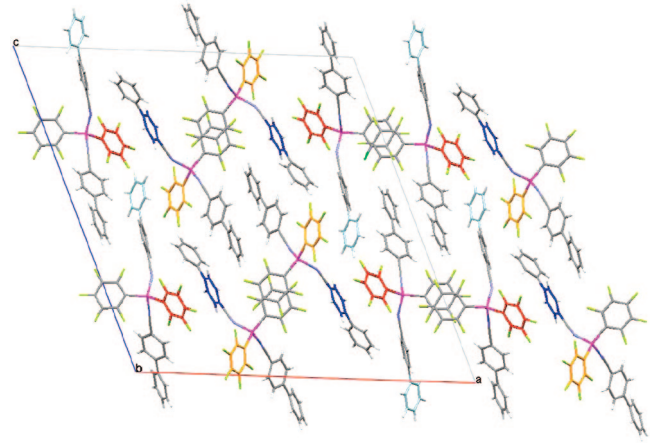

Figure 12. Packing diagram for **2**, viewed along the *b* axis. The aryl ring in dark blue interacts with the red ring (pentafluorophenyl) in a $Ph_F \cdots Ar_H$ interaction, while a second $Ph_F \cdots Ph_H$ interaction occurs between the aryl rings in light blue and the pentafluorophenyl ring in orange.

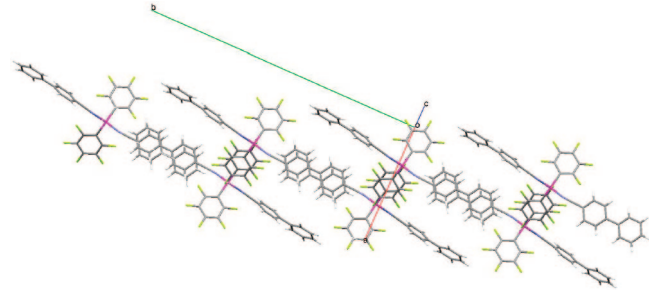

Figure 13. One-Dimensional Network of **2**·(toluene) viewed along the c^* axis.

(22) (a) Renak, M. L.; Bartholemew, G. P.; Wang, S.; Ricatto, P. J.; Lachicotte, R. J.; Bazan, G. C. *J. Am. Chem. Soc* **1999**, *121*, 7787. (b) Gdaniec, M.; Jankowski, W.; Milewska, M. J.; Poloñski, T. *Angew. Chem. Int. Ed.* **2003**, *42*, 3903. (c) El-azizi, Y.; Schmitzer, A.; Collins, S. K. *Angew. Chem. Int. Ed.* **2006**, *45*, 968.

(23) (a) Beck, C. M.; Burdeniuc, J.; Crabtree, R. H.; Rheingold, A. L.; Yap, G. P. A. *Inorg. Chim. Acta* **1998**, *270*, 559. (b) Aspley, C. J.; Boxwell, C.; Buil, M. L.; Higgitt, C. L.; Long, C.; Pertutz, R. N. *Chem. Commun.* **1999**, 1027. For examples of stacking involving C_6F_5 substituents on cyclopentadienyl rings see: (c) Blanchard, M. D.; Hughes, R. P.; Concolino, T. E.; Rheingold, A. L. *Chem. Mater* **2000**, *12*, 1604. (d) Thornberry, M. P.; Slebodnick, C.; Deck, P. *Organometallics* **2000**, *19*, 5352. (e) Thornberry, M. P.; Slebodnick, C.; Deck, P. *Organometallics* **2001**, *20*, 920.

(24) (a) For examples with intramolecular interactions involving metal-bonded C_6F_5 groups see: Parks, D. J.; Piers, W. E.; Parvez, M.; Atencio, R.; Zaworotko, M. J. *Organometallics* **1998**, *17*, 1369. (b) Blackwell, J. M.; Piers, W. E.; Parvez, M.; McDonald, R. E. *Organometallics* **2002**, *21*, 1400.

(25) orenzo, S.; Lewis, G. R.; Dance, I. *New J. Chem.* **2000**, *24*, 295.

(26) unter, C. A.; Sanders, J. K. M. *J. Am. Chem. Soc.* **1990**, *112*, 5525.

(27) (a) For acknowledged examples see: Adams, N.; Cowley, A. R.; Dubberley, S. R.; Sealey, A. J.; Skinner, M. E. G.; Mountford, P. *Chem. Commun.* **2001**, 2738. (b) Hair, G. S.; Cowley, A. H.; Gorden, J. D.; Jones, J. N.; Jones, R. A.; Macdonald, C. L. B. *Chem. Commun.* **2003**, 424.

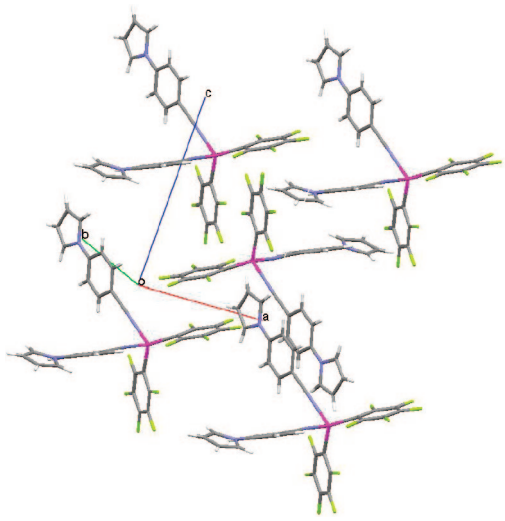

Figure 14. View of the diamondoid packing of **3**, showing the *off* interactions of one molecule with four neighbors.

it is difficult to single out individual attractive contributions. Since every Zn atom lies on a 2-fold symmetry axis which passes through the $\bar{4}$ centers and is parallel to the *c* axis, the supramolecular structure of **5** consists of columns of molecules along this axis connected through the two alternating embraces. Each column is symmetry-related to four others by 2-fold axes parallel to the *a* and *b* axes. Adjacent columns interact through an *off* $Ph_F \cdots Ph_F$ pairing. In addition, the (4-phenyl)pyridine ligands pair through an *off*-like interaction whereby each pyridine ring overlays a phenyl ring (and vice versa).

The lattice of adduct **6** (Figure 7) exhibits essentially the same supramolecular architecture as **5**. Whereas in compound **5** the Zn to Zn distance in the FP_FE is 6.851(2) Å, in this structure the separation between corresponding zinc centers is 7.0058(2) Å.

In adduct **1**, every C_6F_5 (Ph_F) and C_6H_5 (Ph_H) ring is involved in a homoaryl *off* interaction. The major supramolecular motif comprises sheets of $Ph_H \cdots Ph_H$ and $Ph_F \cdots Ph_F$ stacks running parallel to the crystallographic *a* axis, linked through Zn atoms and alternating along *c* (Figure 8). Each sheet is related to the next by a translation in the *b* direction and connected through $Ph_H \cdots Ph_H$ and $Ph_F \cdots Ph_F$ pairing interactions (Figure 9), thus generating a three-dimensional architecture.

The 4-(phenyl)benzonitrile adduct, **2**, crystallizes from dichloromethane solution with two molecules, **2A** and **2B**, in the asymmetric unit. Despite the assembly of the lattice generating two crystallographically distinct molecules, there are a number of close similarities between the intermolecular interactions in which they participate. In both cases one of the pentafluorophenyl rings is part of an infinite *off* $Ph_F \cdots Ph_F$ stack parallel to the *b* axis, each ring along the stack related to the next by a crystallographic 2_1 screw axis (Figure 10). The second C_6F_5 ring of **2A** engages in a pentafluorophenyl−aryl ($Ph_F \cdots Ph_H$) interaction with a *para*-phenyl ring of molecule **2B**: the rings have an interplanar angle of 3.5° and centroid–centroid distance of 3.65 Å (Figure 11b). Between molecules **2B** and **2A**, there is a second $Ph_F \cdots Ph_H$ interaction with an interplanar angle of 19.7° and a centroid–centroid distance of 3.85 Å (Figure 11a). Thus three of the four aryl substituents on each zinc center and one of the outer phenyl rings participate in aryl−aryl intermolecular interactions. In addition, we note that there are two intermolecular C−H···F−C contacts within the van der Waals radii (Table 2).

The supramolecular architecture is built up from two independent columns of molecules linked through the $Ph_F \cdots Ph_F$ stacks. Each column has an equivalent half a unit cell away along the *c* axis. Individual columns of **2A** or **2B** molecules are assembled into a three-dimensional structure by the hetero−aryl interactions (Figure 12).

When **2** crystallizes from toluene as a solvate, its supramolecular structure is quite different from that of the solvent-free analogue. Although, as in **2**, the supramolecular arrangement of **2**·(toluene) is directed by $Ph_F \cdots Ph_F$ and $Ph_H \cdots Ph_H$ *off* interactions, here a one-dimensional chain, linked by alternating offset pentafluorophenyl and offset biphenyl interactions (Figure 13), is formed. Unlike in **2**, there are no pentafluorophenyl−aryl interactions. The two offset C_6F_5 rings are related by an inversion center. One of the 4-(phenyl)benzonitriles on each molecule is also related through an inversion center to an overlapping ligand in an *off* interaction (Figure 15a).

In adduct **3**, there are two pairs of centrosymmetrically related *off* $Ph_F \cdots Ph_F$ interactions (Figure 16c,d). Similarly, each 4-(*N*-pyrrollyl)benzonitrile ligand interacts with another about a center of symmetry such that the phenyl ring of one ligand overlaps the pyrrole ring of the second ligand, and vice versa (Figure 15b). Each of the four ligands thus interacts with a different neighboring molecule, resulting in a three-dimensional diamond-like network (Figure 14). This arrangement includes a short C−H···F−C contact (the F16···H45′ distance is 2.34 Å) between molecules.

Discussion. When we began our investigations into the supramolecular architecture of amine adducts of $(C_6F_5)_2Zn$, we anticipated that the introduction of a phenyl group into the donor would be highly likely to lead to intermolecular quadrupolar phenyl−pentafluorophenyl interactions. In initial results, examining amine adducts, this intermolecular interaction did not predominate, but was found only occasionally in competition with the intramolecular variety, homo−aryl and X−H···F−C interactions.[28]

In this study we have employed ligands without potent X−H hydrogen bond donors. As a result, such interactions do not play a major role in determining the supramolecular architectures described herein. However, some noteworthy C−H···F−C interactions were found, and these are summarized in Table 2. Weak hydrogen-bond-like interactions, such as those present in compound **2**, will make a small, but non-negligible, contribution to directing the assembly of molecules like those studied here, where their significance is enhanced in the absence of

(28) Mountford, A. J.; Lancaster, S. J.; Coles, S. J.; Horton, P. N.; Hughes, D. L.; Hursthouse, M. B.; Light, M. E. *Organometallics* **2006**, *25*, 3837.

(29) Martin, E.; Hughes, D. L.; Lancaster, S. J. *Eur. J. Inorg. Chem.* **2006**, 4037.

(30) Guerrero, A.; Martin, E.; Hughes, D. L.; Kaltsoyannis, N.; Bochmann, M. *Organometallics* **2006**, *25*, 3311.

(31) Horton, A. D.; de With, J.; van der Linden, A. J.; van de Weg, H. *Organometallics* **1996**, *15*, 2672. (b) Duchateau, R.; Cremer, U.; Harmsen, R. J.; Mohamud, S. I.; Abbenhuis, H. C. L.; van Santen, R. A.; Meetsma, A.; Thiele, S. K.-H.; van Tol, M. F. H.; Kranenburg, M. *Organometallics* **1999**, *18*, 5447.

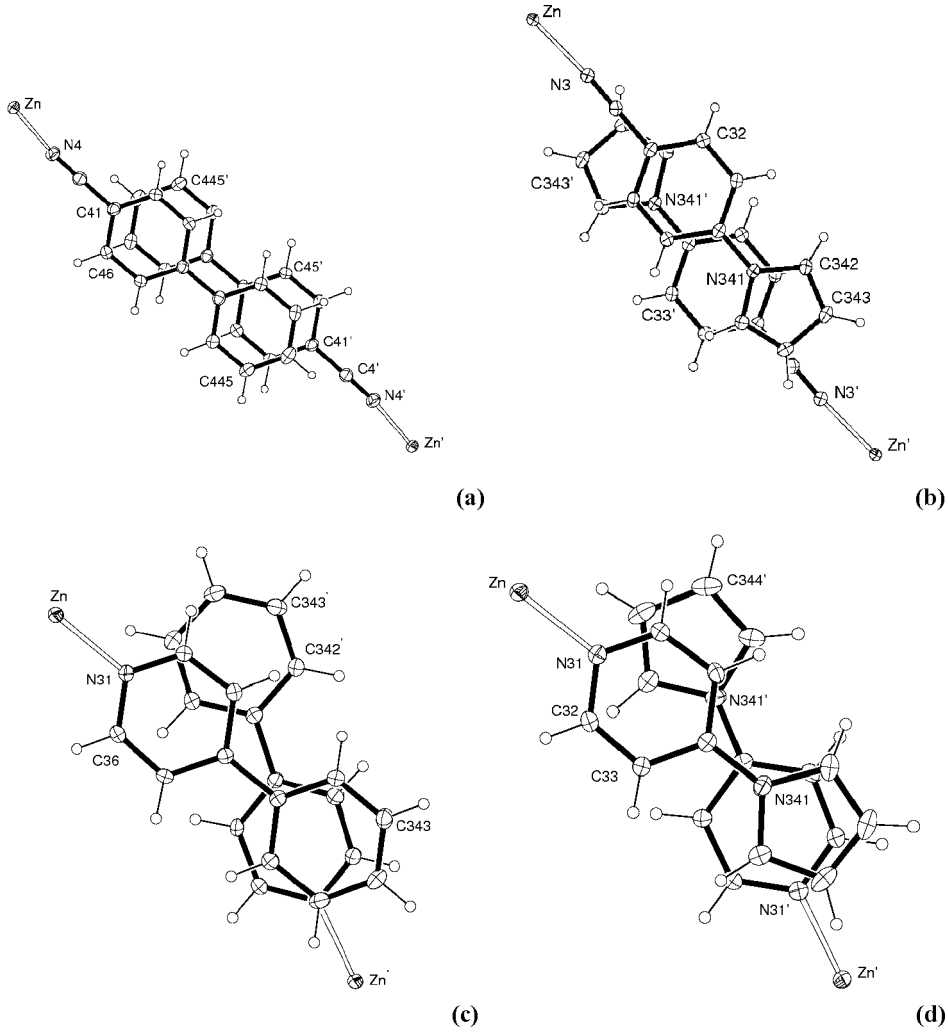

Figure 15. Selected projections of overlapping aromatic rings, ($Ph_H \cdots Ph_H$) (the upper ring is in the plane of the page), for the *off* interactions in **2**·toluene (a), **3** (b), **5** (c), and **6** (d). Displacement ellipsoids are drawn at 30% probability.

stronger interactions.[32] It is also worth noting that the use of rigid benzonitrile or pyridine donors, projecting the phenyl substituent out from the zinc center, has ensured that there are no intramolecular aryl−aryl interactions.

Including the toluene solvate of **2**, six of the seven supramolecular architectures reported here have offset face-to-face interactions between hydrogen-substituted aromatics (*off* $Ph_H \cdots Ph_H$). The variation in the degree of overlap (extent of offset) between selected instances of these interactions is illustrated in Figure 15. Hunter and Sanders have shown that the offset or slipped geometry optimizing $\sigma-\pi$ attractions is the most favorable for face-to-face aryl−aryl interactions.[25] The offset face-to-face interaction is not restricted to single phenyl groups. In **2**·(toluene) (Figure 15a) there is an effective *off* interaction encompassing the whole biphenyl group, while in **3**, **5**, and **6** (Figure 15b,c, and d) the overlap is somewhat less efficient. The centroid–plane distances observed for our *off* homo−aryl series lie in the range 3.41–3.63 Å, which is typical for these interactions.

The offset or slipped geometry has been calculated to again be the most favorable face-to-face arrangement for perfluoroaryl groups.[26] In this series the analogous *off* interaction between pentafluorophenyl rings is equally prevalent in the aryl−aryl and is observed for at least one of the two C_6F_5 groups in six of the seven crystal lattices (selected illustrations are presented in Figure 16). The centroid–plane distances vary between 3.35 and 3.62 Å, and although not as low as that predicted for the gas-phase dimerization of C_6F_6,[26] they are in the same range that we and others have previously reported.[27,28]

In contrast, the only examples of hetero−aryl pairing found in this study were those in the solvent-free supramolecular architecture of **2** (Figure 11). Of these interactions, only that depicted in Figure 11a, between a C_6F_5 ring and the C_6H_4 ring of 4-(phenyl)benzonitrile, shows particularly good overlap. As is typical for hetero−aryl interactions of this type, the rings are somewhat further apart than is the case for homo−aryl contacts: the centroid of the C_6F_5 is 3.84 Å from the plane of the benzonitrile ring, while the C_6H_4 centroid is 3.52 Å from the plane of the C_6F_5 ring.

(32) (a) Borwick, S. J.; Howard, J. A. K.; Lehmann, C. W.; O'Hagan, D. *Acta. Crystallogr., Sect. E* **1997**, *53*, 124. (b) Weiss, H.-C.; Boese, R.; Smith, H. L.; Haley, M. M. *Chem. Commun.* **1997**, 2403. (c) Thalladi, V. K.; Weiss, H.-C.; Bläser, D.; Boese, R.; Nangia, A.; Desiraju, G. R. *J. Am. Chem. Soc.* **1998**, *120*, 8702. (d) Pham, M.; Gdaniec, M.; Poloński, T. *J. Org. Chem.* **1998**, *63*, 3731. (e) Barbarich, T. J.; Rithner, C. D.; Miller, S. M.; Anderson, O. P.; Strauss, S. H. *J. Am. Chem. Soc.* **1999**, *121*, 4280. For estimates of the strength of O−H···F−C hydrogen bonds see: (f) Takemura, H.; Kotoku, M.; Yasutake, M.; Sinmyozu, T. *Eur. J. Org. Chem.* **2004**, 2019. (g) Caminanti, W.; Melandri, S.; Maris, A.; Ottaviani, P. *Angew. Chem. Int. Ed.* **2006**, *45*, 2438, and references therein. For a discussion of weakly attractive C−H···F−C interactions in polymerization catalysis see: (i) Chan, M. C. W.; Kui, S. C. F.; Cole, J. M.; McIntyre, G. J.; Matsui, S.; Zhu, N.; Tam, K.-H. *Chem.−Eur. J.* **2006**, *12*, 2607.

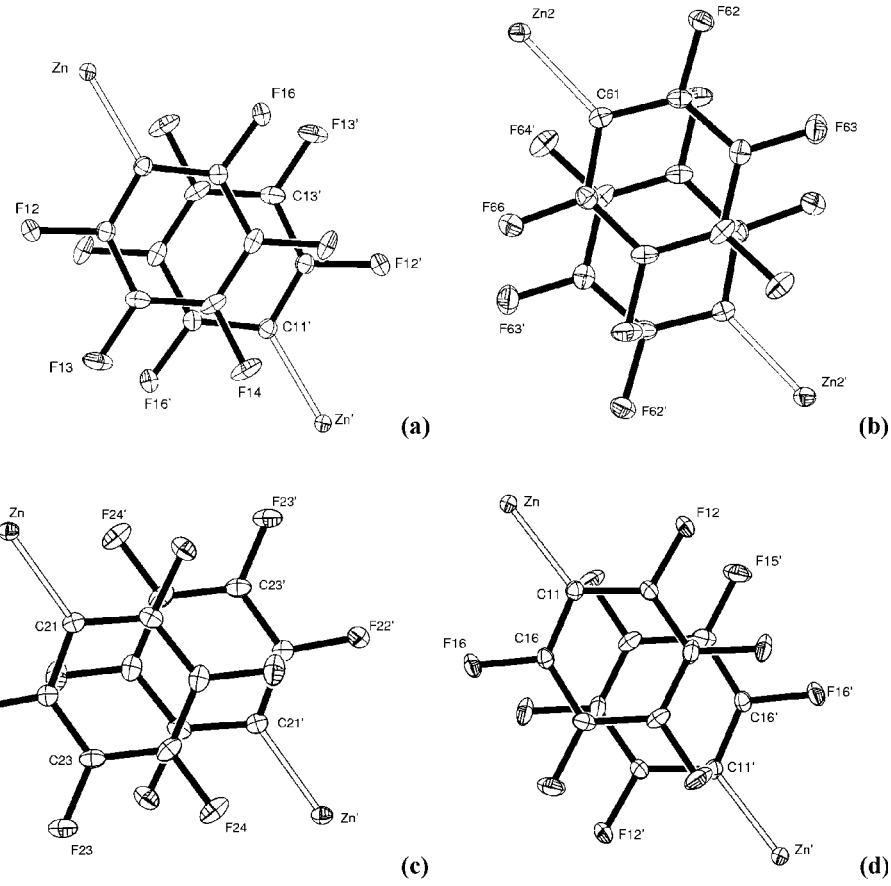

Figure 16. Selected projections of overlapping $Ph_F \cdots Ph_F$ rings (the upper ring is in the plane of the page) in **1** (a), **2** (b), and **3** (c, d). Displacement ellipsoids are drawn at 30% probability.

Despite the fact that the hetero−aryl interaction has been estimated to be potentially twice as strong an attraction, the preference of these complexes for assembly through the offset face-to-face homo−aryl rather than $Ph_F \cdots Ar_H$ hetero−aryl supramolecular synthons is easily rationalized. An effective quadrupolar aryl−perfluoroaryl interaction requires one ring to sit almost directly above the other.[26] Clearly the zinc substituent presents a steric impediment to this arrangement. The 4-pyrrolyl substituent, as well as being more electron-rich, was intended to reduce this steric congestion through the smaller ring size and the absence of a projecting *para* group. Evidently, this strategy was not successful. The *off* interactions avoid the steric constraints imposed by the metal complex and therefore predominate.

The solid-state structures of compounds **1**−**6** provide a number of instances where it is readily apparent that the variation in bond angles observed is as much a consequence of the supramolecular as the coordination chemistry. The anomalously acute C−Zn−C angles in **5** and **6** result from the attractive interactions of the FP_FE embrace and the adoption of an optimal geometry to accommodate the four *off* interactions in which each molecule participates. The observed variation in individual Zn−N−C bond angles for coordinated benzonitrile ligands (Table 1) can also be attributed to supramolecular influences. There is a considerable difference between the Zn−N3−C3 (171.8(2)°) and Zn−N4−C4 (156.66(2)°) angles in compound **1**. Both the phenyl rings are engaged in *off* interactions. However, it is apparent that there is a trade-off between optimal Zn−N−C angle and *off* overlap, such that, if Zn−N4−C4 were more linear, the offset would be much less favorable.

The three distinct molecular structures we have determined for the 4-(phenyl)benzonitrile adduct (**2**) provide a further example of the influence of supramolecular structure on observed molecular geometry. The differences between the C−Zn−C angles in molecules **2A** and **2B**, which are the largest in this series, result from contrasting $Ph_F \cdots Ar_H$ interactions, while **2**·(toluene), in which there is no $Ph_F \cdots Ar_H$ interaction, has a significantly smaller value.

Conclusions

Bis(pentafluorophenyl)zinc forms essentially tetrahedral adducts with 2 equiv of a broad range of nitrogen donors. The benzonitrile and pyridine complexes studied here retain their four-coordinate characters in solution. In the solid state their supramolecular architectures are largely assembled through face-to-face intermolecular interactions between the aromatic groups. The results reported here suggest that homo−aryl offset face-to-face interactions of the type $Zn-Ph_F \cdots Ph_F$ are favored over hetero−aryl, $Zn-Ph_F \cdots Ar_H$. This reflects the steric role of the zinc substituent, which impedes efficient face-to-face hetero−aryl overlap, apparently even with the electron-rich five-membered pyrrolyl ring. In contrast, the offset homo−aryl face-to-face interaction can readily accommodate the zinc substituent and therefore predominates.

Although Zn−C and Zn−N bond lengths show little dependence on the nature of the donor, the distorted tetrahedral geometry varies considerably between ostensibly similar molecular species. These geometrical variations can be traced to the supramolecular architectures, or, put alternatively, these systems display substantial packing effects.

Table 3. Crystal Data and Refinement Results for All Samples

	1	**2**	**2·tol**	**3**[29]	**4**	**5**	**6**
empirical formula	$C_{26}H_{10}F_{10}N_2Zn$	$C_{38}H_{18}F_{10}N_2$ Zn	$C_{38}H_{18}F_{10}N_2$ Zn, $0.5(C_7H_8)$	$C_{34}H_{16}F_{10}N_4Zn$	$C_{22}H_{10}F_{10}N_2Zn$	$C_{34}H_{18}F_{10}N_2Zn$	$C_{30}H_{16}F_{10}N_4Zn$
fw/g mol^{-1}	605.7	757.9	804.0	735.9	557.7	709.9	687.8
cryst syst, space group	triclinic, $P\bar{1}$	monoclinic, $P2_1/c$	monoclinic, $C2/c$	triclinic, $P\bar{1}$	monoclinic, $P2_1/c$	tetragonal, $I\bar{4}2d$	tetragonal, $I\bar{4}2d$
a/Å	7.1098(7)	31.3419(6)	13.480(3)	8.0378(5)	16.1446(9)	17.399(3)	17.2349(3)
b/Å	12.5886(14)	6.7316(1)	30.713(6)	14.0455(7)	10.2398(7)	17.399(3)	17.2349(3)
c/Å	14.7792(19)	32.0060(6)	16.796(3)	14.5510(9)	13.2794(6)	19.300(4)	19.0106(5)
α/deg	68.372(10)	90	90	114.357(6)	90	90	90
β/deg	77.100(8)	112.570(1)	98.45(3)	91.807(5)	106.979(4)	90	90
γ/deg	76.065(9)	90	90	97.603(5)	90	90	90
vol/Å^3	1180.1(2)	6235.5(2)	6878(2)	1476.60(15)	2099.6(2)	5842.6(19)	5646.9(2)
Z, calc density (Mg m^{-3})	2, 1.705	8, 1.615	8, 1.553	2, 1.655	4, 1.764	8, 1.614	8, 1.618
abs coeff (mm^{-1}) μ	1.139	0.880	0.803	0.928	1.271	0.933	0.965
color, habit	colorless blades	colorless needles	colorless slab	colorless prisms	colorless block	colorless plates	colorless irregular blocks
cryst dimens/mm^3	$0.50 \times 0.10 \times 0.04$	$0.20 \times 0.02 \times 0.02$	$0.35 \times 0.20 \times 0.05$	$0.59 \times 0.33 \times 0.30$	$0.30 \times 0.30 \times 0.18$	$0.20 \times 0.12 \times 0.02$	$0.21 \times 0.17 \times 0.15$
θ range (deg)	3.0 to 27.5	2.9 to 27.5	3.0 to 27.5	3.8 to 25.0	3.1 to 27.5	3.2 to 27.5	3.2 to 25.0
no. of reflns collected/unique/obsd	22 063/5403/4515	75 561/14 116/9625	47 440/7850/5730	16 139/5174/4726	24 806/4811/4156	21 900/3355/2847	30 371/2491/2103
R_{int}	0.036	0.110	0.050	0.022	0.027	0.061	0.071
absorption T_{min}/T_{max}	0.600/0.956	0.844/0.983	0.766/0.961	0.914/1.049	0.702/0.804	0.835/0.982	0.870/1.250
no. of data/restraints/params	5403/0/352	14 116/0/919	7850/0/493	5174/0/442	4811/0/317	3355/0/213	2491/0/204
final R indices [$F^2 > 2\sigma(F^2)$]: R_1, wR_2	0.033, 0.077	0.077, 0.091	0.042, 0.101	0.023, 0.062	0.027, 0.069	0.036, 0.065	0.029, 0.044
R indices (all data) : R_1, wR_2	0.047, 0.082	0.131, 0.104	0.070, 0.100	0.026, 0.063	0.035, 0.072	0.051, 0.068	0.043, 0.050
largest diff peak and hole/e Å^{-3}	0.44 and −0.42	0.40 and −0.45	0.39 and −0.47	0.36 and −0.28	0.41 and −0.37	0.19 and −0.28	0.19 and −0.26

We are currently exploring approaches that either utilize the propensity toward offset face-to-face interactions of the M−C_6F_5 group or provide a more favorable steric environment for the $Ar_F \cdots Ar_H$ supramolecular synthon, in order to direct the assembly of related organometallics.

Experimental Section

General Procedures. Syntheses were performed under nitrogen using standard Schlenk techniques. Solvents were distilled over sodium-benzophenone (diethyl ether, tetrahydrofuran), sodium (toluene), sodium−potassium alloy (light petroleum, bp 40–60 °C), or CaH_2 (dichloromethane, 1,2-difluorobenzene). NMR solvents ($CDCl_3$, C_6D_6, C_7D_8) were dried over activated 4 Å molecular sieves and degassed by several freeze−thaw cycles. NMR spectra were recorded using a Bruker DPX300 spectrometer. Chemical shifts are reported in ppm and referenced to residual solvent resonances (^{1}H, ^{13}C); ^{19}F is relative to $CFCl_3$. Elemental analyses were performed by the in-house service at the University of East Anglia or at the Department of Health and Human Sciences, London Metropolitan University. $(C_6F_5)_2$Zn(toluene), 4-(*N*-pyrrolyl)pyridine, and 4-(*N*-pyrrolyl)benzonitrile were prepared according to the literature procedures.[33,34] The remaining benzonitriles and pyridines were purchased from Aldrich or Lancaster, dried over 4 Å molecular sieve, and used without further purification.

Crystal Structure Analyses. Suitable crystals were selected and data for **1**, **2**, **2**·C_7H_8, **4**, and **5** were measured at 120 K at the National Crystallography Service on a Bruker Nonius KappaCCD area detector equipped with a Bruker Nonius FR591 rotating anode ($\lambda_{Mo-K\alpha}$ = 0.71073 Å) driven by COLLECT[35] and processed by DENZO[36] software. For **3** and **6**, data were collected at 140 K at UEA on an Oxford Diffraction Xcalibur-3 CCD diffractometer equipped with Mo Kα radiation and graphite monochromator, and the data were processed using the CrysAlis-CCD and -RED[37] programs. The structures were determined with SHELXS-97 and refined using SHELXL-97.[38] Crystal data and refinement results for all samples are collated in Table 3.

General Procedure for the Synthesis of Adducts 1−7. A solution of $(C_6F_5)_2$Zn·(toluene) (0.50 g, 1.0 mmol) in toluene (10 mL) was treated with the corresponding ligand. The reaction mixture was stirred for 10 min at room temperature before removing the volatiles under reduced pressure, yielding the crude solid.

$(C_6F_5)_2Zn(NCC_6H_5)_2$ (1). 1 was prepared following the general procedure outline above, using benzonitrile (0.21 mL, 2 mmol). The crude solid was crystallized from toluene at –25 °C, affording colorless blade-like crystals of **1** (0.54 g, 0.89 mmol, 89%) suitable for X-ray analysis. ^{1}H NMR (300 MHz, 293 K, C_6D_6): δ 6.90 (dd, 2H, J = 7.8 and 1.3 Hz, *o-H*), 6.73 (tt, 2H, J = 7.6 and 1.3 Hz, *p-H*), 6.51 (dd, 4H, J = 7.8 and 7.6 Hz, *m-H*). ^{19}F NMR (282 MHz, 293 K, C_6D_6): δ –118.1 to –118.2 (m, 4F, *o-F*), –157.94 (t, 2F, J = 20 Hz, *p-F*), –162.40 to –162.66 (m, 4F, *m-F*). Anal. Found: C, 51.03; H, 1.41; N, 4.57. Calc for $C_{26}H_{10}F_{10}N_2Zn$: C, 51.55; H, 1.66; N, 4.62.

$(C_6F_5)_2Zn(NCC_6H_4C_6H_5)_2$ (2). 2 was prepared in a similar fashion to **1**, using 4-(phenyl)benzonitrile (0.36 g, 2 mmol). The

(33) (a) Sun, Y.; Piers, W. E.; Parvez, M. *Can. J. Chem* **1998**, *76*, 513. (b) Weidenbruch, M.; Herrndorf, M.; Schäfer, A.; Pohl, S.; Saak, W. *J. Organomet. Chem.* **1989**, *361*, 139. (c) Day, V. W.; Campbell, D. H.; Michejda, C. J. *J. Chem. Soc., Chem. Commun.* **1975**, 118. (d) Garratt, S.; Guerrero, A.; Hughes, D. L.; Bochmann, M. *Angew. Chem. Int. Ed.* **2004**, *43*, 2166.

(34) Sanchez, I.; Pujol, J. K. *Tetrahedron* **1999**, *55*, 5593.

(35) Hooft, R., Nonius, B. V. *COLLECT*: Data collection software; 1998.

(36) Otwinowski, Z.; Minor, W. *Methods Enzymol.* **1997**, *276*, 307.

(37) Programs *CrysAlis-CCD* and *-RED*; Oxford Diffraction Ltd.: Abingdon, UK, 2005.

(38) Sheldrick, G. M. S*HELX-97*, Programs for crystal structure determination (SHELXS) and refinement (SHELXL); University of Göttingen: Germany, 1997.

crude solid was crystallized by diffusion of petroleum ether in dichloromethane at 2 °C, affording crystals of **2** as colorless needles (0.54 g, 0.71 mmol, 71%) suitable for X-ray analysis. ^{1}H NMR (300 MHz, 293 K, C_6D_6): δ 7.12 to 7.07 (m, 10H), 7.03 (dd, 4H, J = 6.6 and 1.9 Hz), 6.90 (dd, 4H, J= 6.6 and 1.9 Hz). ^{19}F NMR (282 MHz, 293 K, C_6D_6): δ –118.2 to –118.4 (m, 4F, *o-F*), −157.4 (t, 2F, J= 20 Hz, *p-F*), −162.1 to −162.4 (m, 4F, *m-F*). Anal. Found: C, 60.16; H, 2.27; N, 3.79. Calc for $C_{38}H_{18}F_{10}N_2Zn$: C, 60.21; H, 2.39; N, 3.70.

Crystals of **2**·$(C_7H_8)_{0.5}$ suitable for X-ray diffraction were obtained as colorless slabs by cooling a toluene solution of **2** to –25 °C overnight.

$(C_6F_5)_2Zn(NCC_6H_4NC_4H_4)_2$ (3). A solution of $(C_6F_5)_2$Zn-(toluene) (0.44 g, 0.9 mmol) in toluene (10 mL) was treated with 4-(*N*-pyrollyl)benzonitrile (0.30 g, 1.8 mmol). The reaction mixture was stirred for 30 min before being filtered to separate a small amount of solid material. The volatiles were removed under reduced pressure, and the crude solid was crystallized from a mixture of 1,2-difluorobenzene and light petroleum at 2 °C, affording colorless prisms of **3** (0.65 g, 0.88 mmol, 98%) suitable for X-ray analysis. ^{1}H NMR (300 MHz, 293 K, C_6D_6): δ 6.91 (dd, 4H, J = 7.0 and 1.6 Hz, *H* benzonitrile), 6.56 (t, 4H, J = 2.1 Hz, *H* pyrrole), 6.43 (dd, 4H, J = 7.0 and 1.6 Hz, *H* benzonitrile), 6.28 (t, 4H, J = 2.1 Hz, *H*pyrrole). ^{19}F NMR (282 MHz, 293 K, C_6D_6): δ –118.3 to –118.5 (m, 4 F, *o-F*), –157.4 (t, 2 F, J = 19.6 Hz, *p-F*), –162.2 to –162.4 (m, 4 F, *m-F*). Anal. Found: C, 54.94; H, 2.14; N, 7.91. Calc for $C_{34}H_{16}F_{10}N_4Zn$: C, 55.49; H, 2.19; N, 7.61.

$(C_6F_5)_2Zn(NC_5H_5)_2$ (4). 4 was prepared utilizing the general procedure, using pyridine (0.15 mL, 2 mmol). The crude solid was crystallized from toluene at –25 °C, affording colorless block-like crystals of **4** (0.51 g, 0.92 mmol, 92%) suitable for X-ray analysis. ^{1}H NMR (300 MHz, 293 K, C_6D_6): δ 8.16 to 8.13 (m, 4H, *o-H*), 6.82 to 6.75 (m, 2H, *p-H*), 6.46 to 6.42 ppm (m, 4H, *m-H*). ^{19}F NMR (300 MHz, 293 K, C_6D_6): δ –116.4 to –116.5 (m, 4F, *o-F*), –157.6 (t, 2F, J = 19 Hz, *p-F*), –161.9 to –162.2 (m, 4F, *m-F*). Anal. Found: C, 51.03; H, 1.41; N, 4.57. Calc for $C_{22}H_{10}F_{10}N_2Zn$: C, 51.55; H, 1.66; N, 4.67.

$(C_6F_5)_2Zn(NC_5H_4C_6H_5)_2$ (5). Using the general procedure, $(C_6F_5)_2$Zn(toluene) was treated with 4-(phenyl)pyridine (0.31 g, 2 mmol). The crude solid was crystallized from toluene at –25 °C, affording crystals of **5** as colorless plates (0.62 g, 0.87 mmol, 87%) suitable for X-ray analysis. ^{1}H NMR (300 MHz, 293 K, C_6D_6): δ 7.12 to 7.09 (m, 10H), 7.03 (dd, 4H, J = 6.7 and 1.4 Hz), 6.89 (dd, 4H, J = 6.7 and 1.4 Hz). ^{19}F NMR (282 MHz, 293 K, C_6D_6): δ –118.2 to –118.4 (m, 4F, *o-F*), 157.4 (t, 2F, J = 20 Hz, *p-F*), –162.1 to –162.4 (m, 4F, *m-F*). Anal. Found: C, 57.29; H, 2.40; N, 3.90. Calc for $C_{34}H_{18}F_{10}N_2Zn$: C, 57.53; H, 2.57; N, 3.95.

$(C_6F_5)_2Zn(NC_5H_4NC_4H_4)_2$ (6). 6 was prepared following the general procedure, adding 4-(*N*-pyrrollyl)pyridine (0.29 g, 2 mmol). The crude solid was crystallized from a mixture of dichloromethane and petroleum ether (6:1) at –25 °C, affording crystals of **6** as colorless blocks (0.65 g, 0.94 mmol, 94%) suitable for X-ray analysis. ^{1}H NMR (300 MHz, 293 K, C_6D_6): δ 8.08 (dd, 4H, J = 5.3, 1.6 Hz, *H* pyridine), 6.61 (t, 4H, J = 2.2 Hz, *H* pyrrole), 6.33 (dd, 4H, J = 5.3, 1.6 Hz, *H* pyridine), 6.23 (t, 4H, J= 2.2 Hz, *H* pyrrole). ^{19}F NMR (282 MHz, 293 K, C_6D_6): δ –115.9 to –116.2 (m, 4F, *o-F*), –157.4 (t, 2F, J = 20 Hz, *p-F*), –161.7 to –162.0 (m, 4F, *m-F*). Anal. Found: C, 52.57; H, 2.40; N, 8.12. Calc for $C_{30}H_{16}F_{10}N_4Zn$: C, 52.39; H, 2.34; N, 8.15.

$(C_6F_5)_2Zn(2,2'$-bipy) (7). 7 was synthesized following the general procedure, using 2,2-bipyridine (0.16 g, 1 mmol). The crude solid was crystallized from toluene at –25 °C, affording crystals of **7** (0.49 g, 0.88 mmol, 88%). ^{1}H NMR (300 MHz, 293 K, C_6D_6): δ 8.74 (d, 2H, 5.6 Hz), 6.73−6.76 (m, 2H), 6.48−6.44 (m, 2H). ^{19}F NMR (282 MHz, 293 K, C_6D_6): δ –117.1 to –117.3 (m, 4F, *o-F*), –157.9 (t, 2F, J = 20 Hz, *p-F*), –162.0 to –162.2 (m, 4F, *m-F*). Anal. Found: C, 47.17; H, 1.26; N, 5.13. Calc for $C_{22}H_8F_{10}N_2Zn$: C, 47.55; H, 1.45; N, 5.04.

Acknowledgment. We are grateful to the Engineering and Physical Sciences Research Council for a studentship (A.J.M.) and access to the National Crystallography Service. E.M. thanks UEA for a Ph.D. scholarship and Oxford Diffraction Ltd. for a CASE award.

Supporting Information Available: X-ray crystallographic data in CIF format; ORTEP figures depicting the molecular structure of **2**·toluene, **3**, and **5**; an extended quantitative description of the supramolecular architectures of compounds **1**−**6**; diagrams illustrating the degree of overlap in each occurrence of offset face-to-face aryl−aryl and pentafluoroaryl−pentafluoroaryl interactions. This material is available free of charge via the Internet at http://pubs.acs.org.

OM701127P